Performance Estimation of Model-Based Automatic Target Recognition using Attributed Scattering Center Features *

Hung-Chih Chiang and Randolph L. Moses
Department of Electrical Engineering
The Ohio State University
Columbus, OH 43210-1272
{randy,chiangh}@ee.eng.ohio-state.edu

William W. Irving
Alphatech Inc, Burlington, MA 01803

Abstract

We present a model for classification performance estimation for synthetic aperture radar (SAR) automatic target recognition. We adopt a model-based approach, in which classification is performed by comparing a feature vector extracted from a measured SAR image chip with a feature vector predicted from a hypothesized target class and pose. The feature vectors are compared using a Bayes likelihood match metric that incorporates uncertainty in both the predicted and extracted feature vectors. The feature vectors parameterize dominant scattering centers on the target, and include attributes that characterize frequency and angle dependence of scattering centers. We develop Bayes matchers that incorporate two different feature correspondence methods. Finally, we compare performance using measured SAR imagery for a 10-class problem under various match operating scenarios.

1. Introduction

We consider the problem of Automatic Target Recognition (ATR) from synthetic aperture radar (SAR) imagery. SAR target recognition is challenging because of the high variation present in measured imagery. SAR backscatter returns of targets can change significantly with only slight differences in target pose (azimuth and elevation) or target articulation (position of a moving part on the target). As a result, each target class is a highly multimodal composite class with a very large number of dissimilar subclasses. If classification is attempted using template matching, the number of test templates becomes prohibitive in practical problems [4].

*This research was supported in part by DARPA and the Air Force Research Laboratory under Grant F33615-979191020.

To address the dimensionality of the SAR ATR problem, the classification problem is subdivided into stages; a typical three-stage system [6] is shown in Figure 1. The first, prescreener stage performs initial detection of regions of interest (ROIs) that may contain targets of interest. The prescreener is computationally fast and eliminate regions which obviously contain no target. The second, indexer stage operates on regions detected in the first stage, and further reduces non-target false alarms. In addition, the indexer generates a list of candidate target hypotheses, along with a coarse pose estimate for each, often using a coarsely tuned set of templates or features. The coarse estimation is designed to reduce the search space for the final classifier stage. The final classifier is the most computationally intensive process, and estimates the final target class.

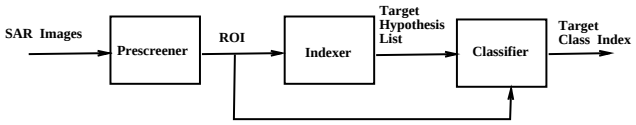

Figure 1. A typical SAR ATR system

The SAR dimensionality problem is also addressed by adopting a model-based approach. In model-based methods, classification is performed by comparing a feature vector extracted from a measured SAR image chip with a feature vector predicted from a hypothesized target class and pose. The feature vectors are compared using a Bayes likelihood match metric that incorporates uncertainty in both the predicted and extracted feature vectors.

The predicted vector is often computed on-line; the prediction engine can be thought of as a black box whose input is the hypothesized target class and pose and whose output is a predicted feature vector, along with feature uncertainty for the prediction. The predicted feature vector is then compared with the feature vector extracted from the SAR region

of interest to determine if there is a match. An example of such a model-based ATR system is the Moving and Stationary Target Acquisition and Recognition (MSTAR) ATR system [2, 8].

In this paper we consider a model-based Bayesian matcher that uses an alternate set of features for SAR ATR. The feature set is based on an *attributed scattering center* model for target scattering [7, 3]. In this model, the backscattered energy present in SAR imagery is modeled as a collection of scattering centers, each characterized by parameters that relate to the physical properties of the scattering mechanism. This paper develops a Bayesian matcher for the attributed scattering center features, based on the work in [2], and presents classification performance results using these features.

2. Attributed Scattering Center Model

At high frequencies, the scattering response of an object is well approximated as a sum of responses from individual scattering centers. These scatterers provide a concise, physically relevant description of the object and are thus good candidates for use in target recognition, radar data compression, and scattering phenomenology studies. We therefore adopt a scattering center-based feature vector for classification.

We use the physically-based attributed scattering model parameterization developed in [3]. The model uses the dominant terms of monostatic scattering solutions from both Physical Optics and the Geometric Theory of Diffraction. The attributed scattering center model assumes that the total scattered field as a function of frequency f and aspect ϕ is a sum of p individual scattering terms:

$$E^s(f,\phi) = \sum_{k=1}^{p} E_k^s(f,\phi) \tag{1}$$

Each scattering center is modeled as

$$\begin{aligned} E_k^s(f,\phi) &= A_k \left(j\frac{f}{f_c}\right)^{\alpha_k} \exp(-2\pi f \gamma_k \sin\phi) \\ &\quad \cdot \text{sinc}\left(\frac{2\pi f}{c} L_k \sin(\phi - \bar{\phi}_k)\right) \\ &\quad \cdot \exp\left(j\frac{4\pi f}{c}(Rx_k \cos\phi + Ry_k \sin\phi)\right) \end{aligned}$$

where (Rx_k, Ry_k) denote the scatterer location, A_k is its amplitude, α_k is its frequency dependence, L_k and $\bar{\phi}_k$ are the length and orientation of distributed scatterers, and γ_k is the aspect dependence of localized scatterers. The scattering model is thus described by the parameter set

$$(A_k, Rx_k, Ry_k, \alpha_k, \gamma_k, L_k, \bar{\phi}_k), \quad k = 1, ..., p \tag{2}$$

Each scattering center is either localized or distributed. For localized scattering centers $L_k = \bar{\phi}_k = 0$ and γ_k characterizes the (mild) aspect dependence of the scattering center; for distributed scattering centers $\gamma_k = 0$ and aspect dependence is described by the pair $(L_k, \bar{\phi}_k)$. The frequency dependence parameter α_k discriminates between flat surface scattering ($\alpha = 1$), singly- or doubly-curved surfaces ($\alpha = 1/2$ or $\alpha = 0$), and diffraction scattering $\alpha <= 0$ [3].

The point scattering model can be seen as a special case of the attributed scattering center model with $\gamma_k = L_k = \alpha_k = 0$. The attributed scattering model generalizes the common point scattering model (which assumes scattering centers are isolated points whose responses are all identical, and are independent of frequency and angle), and thus provides a richer, physically relevant description of scattering behavior.

Algorithms for estimating the scattering model parameters from measured SAR imagery, as well as feature uncertainty and Cramér-Rao uncertainty bounds, are presented in [3, 5].

3. Bayesian Matchers

In this section we derive the Bayes match function used in our analysis. At the input to the classifier stage, we have a given region of interest (a SAR image chip), along with a set $\mathcal{H}$ of candidate target hypotheses $\mathcal{H} = \{H_1, \ldots, H_M\}$, where each hypothesis contains target class and pose. From the image chip we extract a feature vector Y, and from a candidate hypothesis H we predict a feature vector X, where

$$X = [X_1, X_2, \ldots, X_{N_x}]^T, \quad Y = [Y_1, Y_2, \ldots, Y_{N_y}]^T \tag{3}$$

and where N_x, N_y are the number of predicted and extracted scattering centers, respectively. Each X_i and Y_j is a vector of scattering attributes; in this paper we consider a reduced set of features given by

$$(A_k, Rx_k, Ry_k, \alpha_k, L_k), \quad k = 1, ..., p \tag{4}$$

We do not include γ and $\bar{\phi}$ attributes in the model, because we expect these features to have a minor role in target discrimination capability.

3.1. Bayes Likelihoods

The classification goal is to maximize $f(H|Y)$. By Bayes rule we have

$$f(H|Y) = \frac{f(Y|H)f(H)}{f(Y)} \tag{5}$$

We assume $f(H)$ and $f(Y)$ are constant, and seek to maximize $f(Y|H)$. To do so, we model this likelihood by relating Y with its predicted counterpart X. An extracted scattering

center Y_j will either correspond to a predicted scattering center X_i, or be a "false alarm" scatterer due to clutter in the SAR image. If Y_j corresponds to X_i, we find $f(Y_j|H)$ as $\int f(y_j|x_i,H)f(x_i|H)\,dx_i$; otherwise we compute $f(Y_j|H)$ from the clutter density function $f_c(Y_j)$. Thus, we need to have models for $f(Y|X,H)$, $f(X|H)$, and $f_c(Y_j)$.

We assume the X_i are conditionally independent given H, and that Y_j are conditionally independent given H and X. The independence of the X_i is reasonable because the prediction errors of separate scattering centers would be due to variations in components on the target that make up that scattering center, and these variations can be assumed to be unconnected. The independence of the Y_i is supported by the near block diagonality of the CRB matrix for well-separated scattering centers [3]. We further assume that the individual parameters that make up each X_i and Y_j are independent. There is little empirical information exists to either support or contradict an independence assumption, but since the independence assumption simplifies the Bayes matcher significantly, we choose to adopt it until sufficiently compelling evidence becomes available to suggest otherwise. Under these independence assumptions, it suffices to model each feature separately; we denote the "θ" feature in X_i or Y_j, where θ is one of the parameters in equation (4), as $x_{i\theta}$ and $y_{j\theta}$, respectively.

3.2. Likelihood of a Single Feature

For the performance estimation study in this paper, we assume a particular form for the density function $f(x_{i\theta}|H)$. We assume that the location parameters are Gaussian random variables, and that the amplitude parameters are log-normal. We also assume α is Gaussian. We simplify the L parameter as a binary detection of $L=0$ versus $L>0$.

The density functions for extracted features that are due to clutter are modeled as follows. We assume a uniform 2-d Poisson model for clutter location, with an average of λ clutter scattering centers per pixel. The location is uniformly distributed on the target chip. We assume the remaining extracted clutter attributes have the same statistical distribution as target scattering attributes.

Each parameter θ in extracted scattering center feature vector Y_j that corresponds to a predicted scattering center feature vector X_i has a conditional likelihood model $f(y_{j\theta}|x_{i\theta},H)$ as follows. If θ is a location, log amplitude, or α parameter, its conditional likelihood is assumed to be Gaussian, so

$$f(y_{j\theta}|x_{i\theta},H) \sim \mathcal{N}(x_{i\theta},\sigma^2_{j\theta}, \tag{6}$$

For a discrete random variable feature (such as the discrete length statistic), the likelihood is a weighted sum of conditional mass functions

$$\begin{aligned} P(y_{j\theta}|H) &= \sum_{\bar{x}_{i\theta}} P(y_{j\theta}|\bar{x}_{i\theta},H)\ \cdot\ P(\bar{x}_{i\theta}|H) \\ &= \sum_{\bar{x}_{i\theta}} P(y_{j\theta}|\bar{x}_{i\theta})\ \cdot\ P(\bar{x}_{i\theta}|x_{i\theta}) \end{aligned} \tag{7}$$

Further discussion of the uncertainty assumptions can be found in [1].

3.3. Feature Correspondences

In order to compute the likelihood, we must correspond the extracted and predicted feature vectors in some way. An extracted feature vector is not ordered with respect to the corresponding predicted feature vector. In addition, the extracted feature vector may not contain the same number of scattering centers as a predicted feature vector, because the extraction algorithm may fail to detect a scattering center or detect a clutter peak in the SAR image as a scattering center. Missing and spurious scattering centers can happen. This fact increases the difficulty for developing SAR feature-based matchers. We consider two commonly used correspondence mappings below [2]. These two correspondence mappings lead to two different formations of the match likelihood functions.

Many-to-Many Correspondence: Figure 2 shows a correspondence map between a set of predicted scatterers and extracted scatterers. Each extracted scattering center is mapped from every predicted scattering center or clutter with some probability. Let $P_i(H)$ denote the probability of detecting the ith predicted scattering center under hypothesis H, and let λ denote the average number of Poisson clutter scattering centers per chip. Following [2] we have

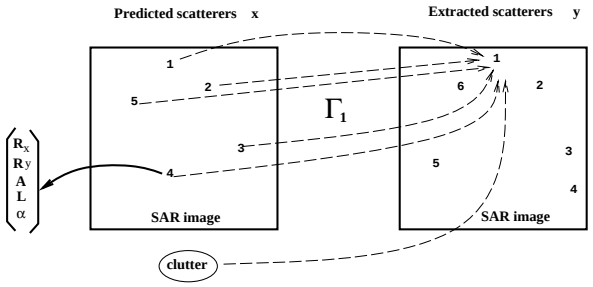

Figure 2. A many-to-many correspondence map between predicted scatterers and extracted scatterers

$$B = \frac{\lambda}{\lambda + \sum_{k=1}^{N_x} P_k(H)} \tag{8}$$

as the probability that the extracted scattering center comes from clutter, and

$$D_i(H) \;=\; (1-B)\frac{P_i(H)}{\sum_{k=1}^{N_x} P_k(H)} \tag{9}$$

as the probability that the extracted scattering center comes from the ith predicted scattering center.

For the many-to-many map, we have

$$f(y|H) \;=\; \prod_{j=1}^{N_y} f(y_j|H) \tag{10}$$

$$\;=\; \prod_{j=1}^{N_y}\left[Bf_c(y_j) + \sum_{i=1}^{N_x} D_i(H) f(y_j|x_i)\right] \tag{11}$$

$$\;=\; \prod_{j}\left[B\prod_{\theta} f_c(y_{j\theta}) + \sum_{i} D_i(H)\prod_{\theta} f(y_{j\theta}|x_{i\theta})\right] \tag{12}$$

We use the independent scattering center assumption in equation (10), use the many-to-many mapping structure described before in equation (11), and use the independent scattering attributes assumption in equation (12).

One-to-One Correspondence: Figure 3 shows a one-to-one correspondence map. Each extracted scattering center can only be mapped from either one of the predicted scattering center or clutter. Let Γ be such a correspondence map.

In this case, Γ can be treated as a random variable which we maximize over, and $f(y, \Gamma|H)$ expression includes missing predicted scattering centers and permutation of clutter scattering centers as

$$f(y,\Gamma|H) \;=\; \exp^{-\lambda}\frac{\lambda^f}{N_x!}\prod_{\{j:\Gamma_j=0\}} f_c(y_j) \cdot \prod_{\{j:\Gamma_j\neq 0\}} P_{\Gamma_j}\int f(y_j|x_{\Gamma_j}) f(x_{\Gamma_j}) dx_{\Gamma_j} \cdot \prod_{\{k:\Gamma_j\neq k,\forall j\}} (1-P_k(H)) \tag{13}$$

where $\Gamma_j = 0$ if y_j is mapped from clutter and $\Gamma_j = i$ if y_j is mapped from x_i, f is the number of clutter scattering centers given by the correspondence map Γ.

3.4. Maximum likelihood Matchers

Let T denote the target class decision by the classifier. The maximum likelihood (ML) matchers are

$$T_{mm} \;=\; \text{ind}\max_{H_i} f(y|H_i), \quad \text{(many-to-many)} \tag{14}$$

$$T_{11} \;=\; \text{ind}\max_{\Gamma, H_i} f(y,\Gamma|H_i), \quad \text{(1-1)} \tag{15}$$

where $f(y|H_i)$ in (14) is given by (12) and $f(y, \Gamma|H_i)$ in (15) is given by (13).

The ML matcher for the one-to-one map requires the search of all possible correspondences Γ. This is computationally more expensive than the ML matcher for the many-to-many map. The many-to-many map has the interpretation of averaging over the likelihoods of all possible one-to-one maps [1]. If the likelihood of the best match is significantly larger than the likelihood of all other matches, the two matchers can be shown to given nearly identical results [1].

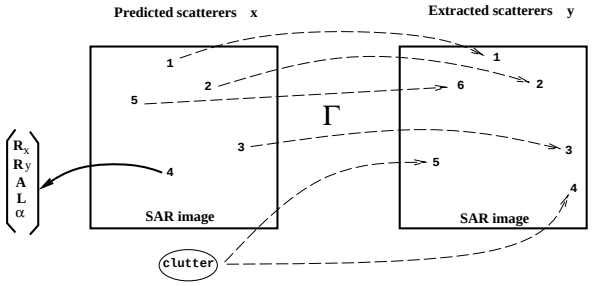

Figure 3. A one-to-one correspondence map between predicted scatterers and extracted scatterers

4. Performance Evaluation

In this section we compare the classification performance results from the Bayesian matcher under a variety of conditions. We propose an evaluation method using feature vector means based on measured SAR imagery, coupled with an assumed feature perturbation model. . We compare performance when using two features (location, amplitude) to performance when using four features (location, amplitude, α, L). We also consider the effect of different scattering center detection probabilities.

4.1. Data and Experimental Procedure

Our simulations are based on features extracted from ten targets in the MSTAR Public Targets dataset. These are X-band image chips with 128x128 pixels and 0.3m$\times$0.3m resolution SAR data chips of ten targets at 17 degree depression angle. For each target approximately 270 images are available covering the full 360 degree aspect angles. There are a total of 2747 images.

Peak features (down/cross range locations and magnitude of peak amplitudes) are extracted from each image chip using a peak extraction routine which essentially finds

local maxima in the SAR image. The remaining parameters were not available, and were generated synthetically. The nominal values of the type attribute are generated as $\alpha \sim \mathcal{N}(0.5, 0.25)$. The nominal values of the length attribute are generated using a Bernoulli random variable with a $P(L > 0) = 0.1$ in (7). These form the 2747 class mean vectors for the 10 composite target classes. The noise perturbations we use on the feature attribute means are:

- For Predicted feature vectors ($f(x_{i\theta}|H)$):
  locations: $\mathcal{N}(0, \sigma^2)$ with $\sigma = 0.3\,\mathrm{m}$
  amplitude: $\log_{10}(|A|) \sim \mathcal{N}(0, 0.25)$
  frequency dependence: α is $N(0, 0.25)$
  length: confusion matrix $= \begin{bmatrix} 1 & 0 \\ 0 & 1 \end{bmatrix}$ (no uncertainty)

- For Extracted feature vectors ($f(y_{j\theta}|x_{i\theta}, H)$):
  locations: $\mathcal{N}(0, \sigma^2)$ with $\sigma = 0.3\,\mathrm{m}$
  amplitude: $\log_{10}(|A|) \sim \mathcal{N}(0, 0.25)$
  frequency dependence: α is $N(0, 0.25)$
  length: confusion matrix $= \begin{bmatrix} 0.8 & 0.2 \\ 0.2 & 0.8 \end{bmatrix}$

- Clutter features
  locations: 2D Poisson with rate $\lambda = 3$ per image chip
  amplitude: $\log_{10}(|A|) \sim \mathcal{N}(\mu, 0.25)$, with
  $\mu = \log_{10}(\text{median ampl of tgt sc ctrs})$
  frequency dependence: $\alpha \sim \mathcal{N}(0.5, 1)$
  length: L is Bernoulli with $P(L > 0) = 0.1$

We emulate the indexer as follows. For each of the 2747 target image chips, we find the 5 image chips in each of the 10 target classes that have the highest correlation with it. The targets classes and poses (pose is in this case azimuth angle) corresponding to these 50 image chips form the initial hypothesis list that is provided to the Bayes classifier.

For each test pattern, we find the 50 hypotheses from the indexer, and generate 10 predicted scattering centers for each hypotheses by randomly perturbing the class means as described above. We similarly generate 10 extracted scattering centers from each realization of the predicted feature vector. The extract feature vectors assume each scattering center has a probability of detection that ranges from $P_d = 0.5$ to 0.9 depending on the experiment; thus, not all scattering centers are present in the extracted feature vector. We also add clutter scattering centers to the extract feature vector. We then compute the one-to-one likelihood function in equation (13) and the many-to-many likelihood function in equation (12) for the extracted scattering center given each hypothesis, and choose the one of the 50 hypotheses with the highest likelihood score. This gives a total of 27,470 classifications from 27,470$\times$50 matches.

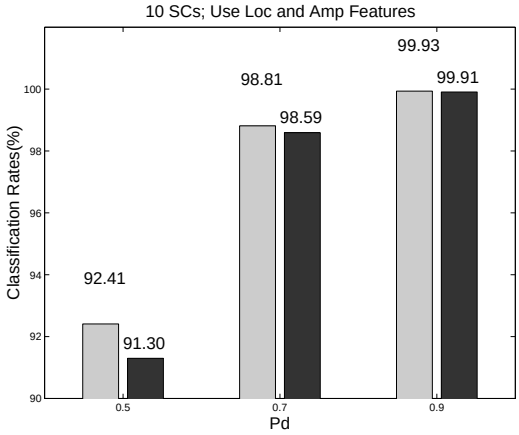

(a) Two attributes

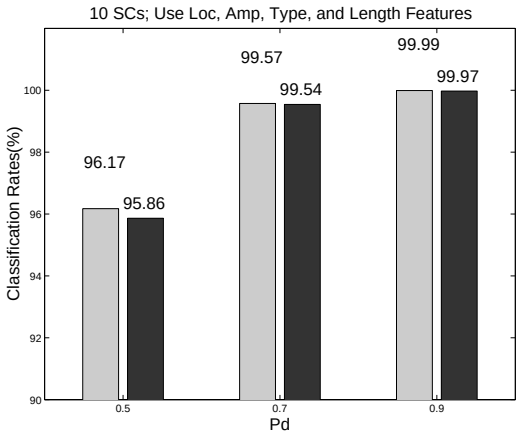

(b) Four attributes

Figure 4. Classification performance using two and four attributes.

4.2. Number of Scattering Attributes

Figure 4 shows the one-to-one and many-to-many classification performance using four and two attributes with $Pd = 0.5, 0.7, 0.9$. We can see that introducing the additional type and length attributes does reduce classification errors by about a factor of two. We also find that the classification performance using a many-to-many matcher is only slightly lower that the classification performance using a one-to-one matcher in this scenario. The one-to-one matcher requires the search for the best correspondence which introduces more computational complexity than the many-to-many matcher which only averages the likelihood scores pointwise. The many-to-many matcher was 2-4 times faster for this example, and the speed ratio increases linearly with the number of scattering centers to be matched.

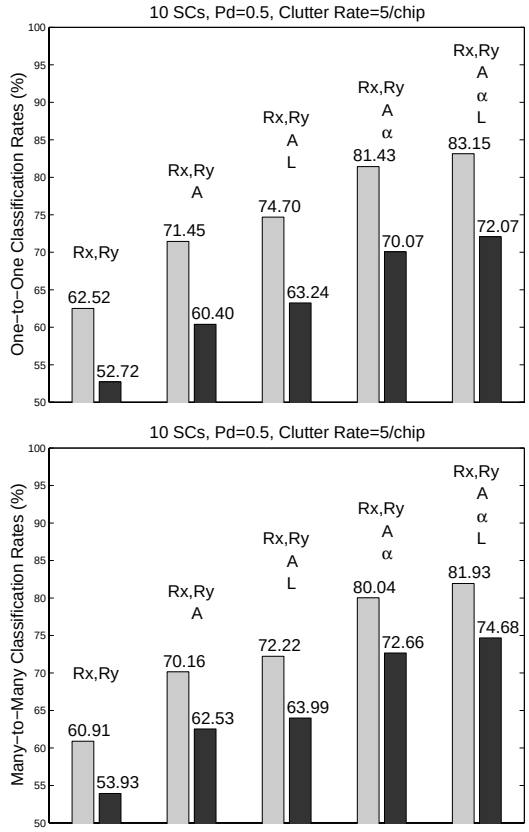

Figure 5. Classification performance on stability of detecting target scattering centers

4.3. Scattering Center Stability

In this experiment we study the effects of stability of target scattering centers. We use ten scattering centers per target chip with a P_d of 0.5 and on average 5 clutter scattering centers per chip. Clutter scattering centers are distributed only on a rectangular target mask to emulate unmodeled scattering on the target region. The low detection probability of scatterers emulates a situation in which scattering centers "scintillate" and may not be detectable at slight pose offsets from the predicted pose. We compare classification performance using two matchers, each with different assumptions on the scattering uncertainty. Matcher 1 use the correct $P_d = 0.5$ and a clutter rate of 5/chip and Matcher 2 erroneously use $P_d = 0.9$ and a clutter rate of 1/chip. Figure (5) summarizes the simulation results.

Compared to the results obtained previously, the correct classification rates are significantly lower in this case, even if the matcher assumes the correct statistical model. This result is expected, since on the target region the clutter scattering centers are confused by target scattering centers by the matchers, leading to higher classification error rates. In addition, the classification performance degrades significantly when the matchers assume $P_d = 0.9$ and a clutter rate of 1/chip. The reason is that the matcher puts too much confidence in good matches of predicted scattering centers to clutter scattering centers extracted from the target. Finally, we see that when the matcher assumes $P_d = 0.9$, many-to-many classifier performed slightly better than the one-to-one classifier. This may be due to a slightly increased robustness of the classifier that results from the averaging over all feature correspondence maps.

5. Conclusions

Our simulation studies show that additional attributes on scattering features show promise for improved SAR classification performance using model-based ATR. The actual degree of improvement depends on the estimation accuracy of the additional features. We found that the the many-to-many matcher performs only slightly worse than the one-to-one matcher (and slightly better in one experiment), but is computationally much less expensive than the one-to-one matcher. Future work is focused on examining the effects of resolution versus performance, and on coupling uncertainty models with prediction and extraction module performance.

References

[1] H.-C. Chiang and R. L. Moses. ATR Performance Prediction Using attributed Scattering Features. In *SPIE*, Orlando, Florida, Apr. 1999.

[2] G. J. Ettinger, G. A. Klanderman, W. M. Wells, and W. E. L. Grimson. A Probabilistic Optimization Approach To SAR Feature Matching. *SPIE*, 2757:318–329, Apr. 1996.

[3] M. Gerry. *Two-dimensional Inverse Scattering Based on the GTD Model*. PhD thesis, The Ohio State University, Columbus, OH, 1997.

[4] E. R. Keydel, S. W. Lee, and J. T. Moore. MSTAR Extended Operation Conditions. *SPIE*, 2757:228–242, Apr. 1996.

[5] M. Koets. Automated Algorithms for Extraction of Physically Relevant Features from Synthetic Aperture Radar Imagery. Master's thesis, The Ohio State University, Columbus, OH, 1998.

[6] L. M. Novak, G. J. Owirka, and C. M. Netishen. Radar Target Identification Using Spatial Matched Filters. *Pattern Recognition*, 27(4):607–617, 1994.

[7] L. C. Potter and R. L. Moses. Attributed Scattering Centers for SAR ATR. *IEEE Trans. Image Processing*, 6(1):79–91, Jan. 1997.

[8] J. Wissinger, R. Washburn, D. Morgan, C. Chong, N. Friedland, A. Nowicki, and R. Fung. Search Algorithms For Model-Based SAR ATR. *SPIE*, 2757:279–293, Apr. 1996.